tissue fibrosis associated with aging (Brack et al., 2007). We examined the effects of C1q treatment on skeletal muscle satellite cells and fibroblasts because these cell types play important roles during skeletal muscle regeneration, the former being the source of new myocytes and the latter being responsible for fibrotic change of the regenerating tissue. We isolated satellite cells and fibroblasts from skeletal muscle of young mice and treated them with C1q or Wnt3A. Both treatments stabilized cytosolic β-catenin (Figure 6A) and increased *Axin2* gene expression (Figure S4A) in these cell types. Serum from aged mice also stabilized cytosolic β-catenin and increased *Axin2* gene expression more potently than serum from young mice, and this effect of serum from aged mice was inhibited by M241 (Figures 6B and S4B). These results suggest that C1q activates Wnt signaling both in satellite cells and fibroblasts and that C1q accounts for increased Wnt signaling activation by serum from aged mice in these cells.

We also tested whether C1q activates Wnt signaling in skeletal muscle in vivo using TOPGAL mice, which express β-galactosidase (β-gal) transgene under the control of Tcf/Lef-binding sites. For C1q application, we placed hydrogel containing C1q on the gastrocnemius muscle. Interestingly, C1q treatment alone did not activate Wnt signaling in skeletal muscle of young mice. However, 2 days after cryoinjury, Wnt signaling activity was slightly increased in injured skeletal muscle of control mice and was robustly enhanced in mice treated with C1q (Figures 6C and 6D). Real-time PCR analysis revealed that the expressions of *C1r* and *C1s*, but not *lrp5* or *lrp6*, were markedly upregulated after injury (Figure 6E), suggesting that induction of C1r and C1s contributes to the enhanced Wnt signaling activation by C1q in injured muscle.

We next examined the effect of C1q-induced activation of Wnt signaling on satellite cells and fibroblasts derived from skeletal muscle in vitro. We found that C1q and Wnt3A attenuated satellite cell proliferation, whereas they stimulated fibroblast proliferation (Figures 6F and 6G). C1q and Wnt3A also increased the collagen production/release from fibroblasts (Figure 6H). Likewise, serum from aged mice attenuated satellite cell proliferation, stimulated fibroblast proliferation, and increased collagen production in fibroblasts, and these effects were abolished by M241 treatment (Figures 6I–6K). We also found that C1q treatment decreased the number of proliferating satellite cells and increased the number of proliferating fibroblasts in skeletal muscle in vivo (Figures 6L, 6M, S4C, and S4D). Taken together, reduced regenerative capacity associated with increased fibrosis in the skeletal muscle of aged organisms may be explained by differential effects of C1q-induced activation of Wnt signaling on satellite cells and fibroblasts.

C1q Mediates Impaired Skeletal Muscle Regeneration Associated with Aging

We then examined whether C1q mediates reduced regenerative capacity of skeletal muscle associated with aging. When the gastrocnemius muscle of young mice was cryoinjured and treated with C1q, canonical Wnt signaling was activated (Figure 7A). C1q treatment also strongly impaired regeneration and promoted fibrotic change in skeletal muscle (Figure 7B). Enhanced tissue fibrosis was also evidenced by increased expression of *Col3a1* gene and increased soluble collagen content in the regenerating muscle (Figures 7C and 7D). Activation of Wnt signaling and impairment of skeletal muscle regeneration after C1q treatment was also observed in C3-deficient mice (Figures 7A–7D), suggesting that the effect of C1q treatment on skeletal muscle regeneration is independent of the classical complement pathway activation.

We also cryoinjured the gastrocnemius muscle of aged wild-type and C1qa-deficient mice and placed the hydrogel containing either M241 or an anti-C5 antibody (BB5.1) that prevents the cleavage of C5. The former inhibits C1s and blocks both C1q-induced activation of Wnt signaling and the activation of the classical complement pathway, whereas the latter selectively blocks the classical complement pathway. C1s inhibition or *C1qa* gene disruption, but not the inhibition of complement activation, attenuated Wnt signaling activity in skeletal muscle and improved skeletal muscle regeneration with reduced tissue fibrosis following cryoinjury on aged mice (Figures 7E–7H). These results suggest that C1q-induced activation of Wnt signaling, but not C1q-triggered classical complement pathway

(C) Western blot analysis of the N-terminal cleaved form of LRP6 in culture media. N-terminal cleaved form of LRP6 was detected in culture media conditioned by cells treated with normal human serum, but not with C1q-depleted serum. Addition of purified C1q protein (100 μg/ml) to C1q-depleted serum restored the activity to cleave LRP6. IgHC, immunoglobulin heavy chain.

(D and E) N-terminal cleaved fragment of LRP6 in the serum was analyzed by western blotting (D) and ELISA (E). In wild-type (WT) mice, the amount of cleaved form of endogenous LRP6 ectodomain was increased by 2-fold in serum from aged mice (2 years old: 130 ng/ml) compared with serum from young mice (2 months old: 60 ng/ml). Cleaved LRP6 was not detected in the serum from young C1qa-deficient mice. Data are presented as mean ±SD.

(F–H) TOPFLASH assay. Overexpression of N-terminal truncated LRP6 (Del-LRP6) resulted in enhanced activation of Wnt signaling compared with wild-type LRP6 (WT-LRP6) (F). Cells transfected with WT-LRP6 responded to both C1q (100 μg/ml) and Wnt3A (10 ng/ml) (G), whereas those transfected with C1s-resistant LRP6 (Mt-LRP6) responded to Wnt3A, but not to C1q (H). Data are presented as mean ±SD.

(I) Western blot analysis of C-terminal LRP6 fragment in the membrane/organelle fraction and N-terminal LRP6 fragment in the culture media after treatment of HepG2 cells with C1q (100 μg/ml). Both C-terminal and N-terminal LRP5/6 fragments were not detected in cells transfected with siRNAs against C1r and C1s (C1r/s), LRP5 and LRP6 (LRP5/6), or cells transfected with Shisa (Shisa O/E). An arrow indicates C-terminal LRP6 fragment, and an arrowhead indicates N-terminal LRP6 fragment.

(J) (Top) β-catenin stabilization assay. HepG2 cells transfected with control siRNA (Con) responded to C1q (100 μg/ml), but those transfected with siRNAs against C1r and C1s (C1r/s), LRP5 and LRP6 (LRP5/6) or cells transfected with Shisa (Shisa O/E) did not. (Bottom) TOPFLASH assay. HEK293 cells transfected with control siRNA responded to both C1q (100 μg/ml) and Wnt3A (10 ng/ml), whereas those transfected with siRNAs against C1r and C1s (C1r/s) responded to Wnt3A, but not to C1q. Data are presented as mean ±SD.

(K) Schematic diagram of C1q-induced activation of Wnt signaling. Upon binding to Fz receptors, C1q activates C1r/C1s, which results in LRP5/6 cleavage and activation of Wnt signaling.

See also Figure S3.

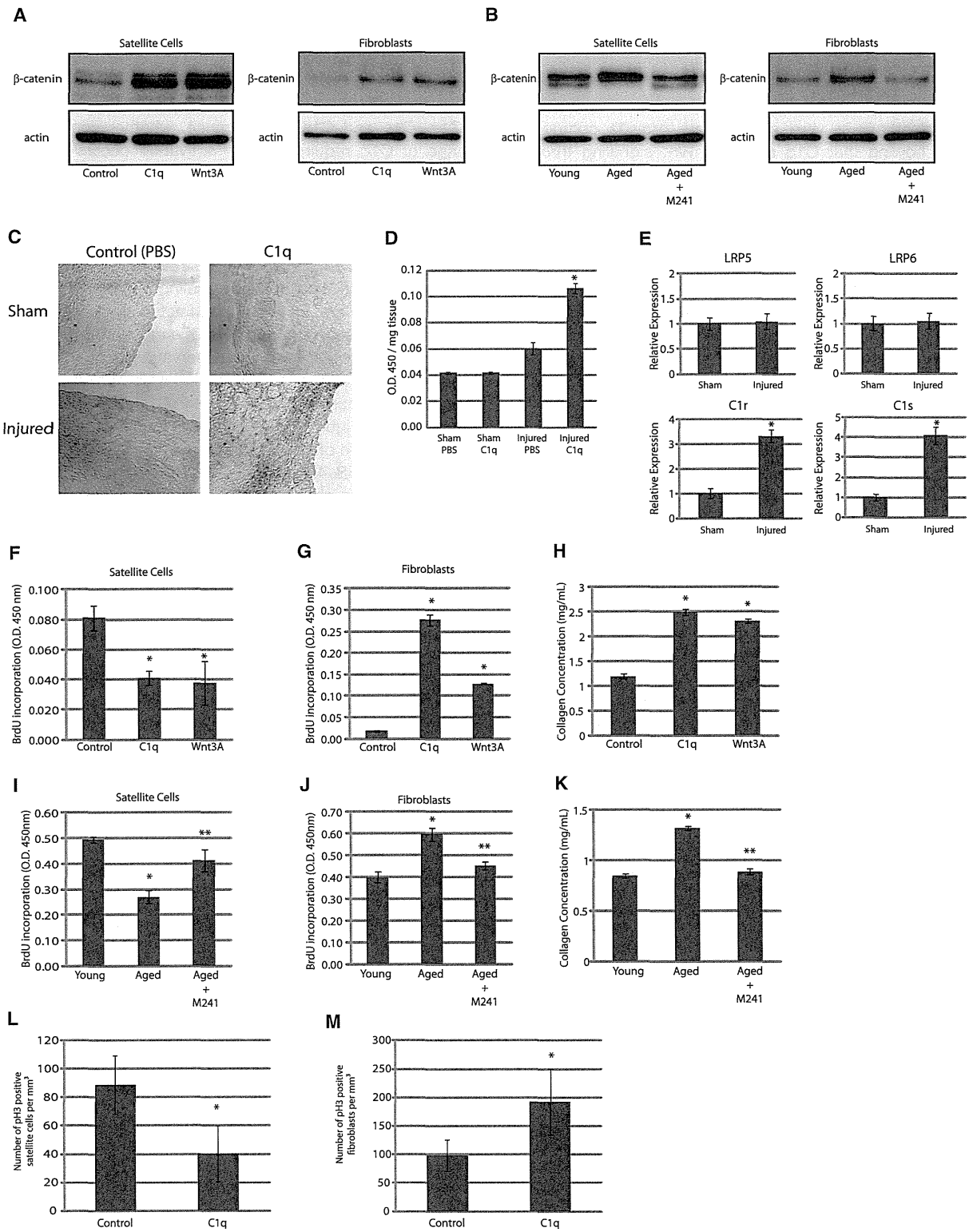

Figure 6. C1q Activates Wnt Signaling in Skeletal Muscle and Exhibits Differential Effects on Satellite Cells and Fibroblasts

(A and B) β-catenin stabilization assay. Satellite cells and fibroblasts were stimulated with C1q (100 μg/ml) or Wnt3A (10 ng/ml). Both C1q and Wnt3A activated Wnt signaling in these cells (A). Cells were also stimulated with serum derived from young (2 months old) or aged mice (2 years old). The extent of Wnt signaling activation by serum from aged mice was greater than that by serum from young mice, and activation of Wnt signaling by serum from aged mice was attenuated by M241.

activation, mediates reduced regenerative capacity in skeletal muscle associated with aging.

DISCUSSION

The results of our in vitro experiments provide compelling evidence showing that C1q activates Wnt signaling through C1s-dependent cleavage of the ectodomain of LRP6 (Figure 5K). The physiological relevance of C1q-induced activation of Wnt signaling in vivo is supported by the following observations. First, an aging-related increase in serum-induced activation of Wnt signaling correlated with an increase in the amount of serum C1q (Figures 1C, 2B, 3A, and 3B), and the concentration of C1q that was shown to activate canonical Wnt signaling in cell culture experiments (100 μg/ml) was within the physiological range of the serum concentration of C1q in humans and mice (Figure 3A) (Borque et al., 1995; Yonemasu et al., 1978). Second, cleaved product of LRP6 was detected in the serum in wild-type mice, but not in C1qa-deficient mice, and its amount was increased with aging (Figures 5D and 5E). Third, the expression of *Axin2* gene was downregulated in various tissues of C1qa-deficient mice, but not of C3-deficient mice (Figure 2G). Fourth, enhanced Wnt signaling activation by serum and increased Wnt signaling in multiple tissues associated with aging were observed in wild-type, but not in C1qa-deficient mice (Figures 2B and 3E). These observations strongly suggest the physiological relevance of C1q-induced activation of Wnt signaling in vivo.

Although C1q and Wnt3A bind to Fz receptors with similar affinity (Figures 1I and S1E), EC_{50} value of C1q on TOPFLASH activity cells was much higher than that of Wnt3A (Figure 1M). In particular, the extent of Wnt signaling activation induced by 100 μg/ml (200 nM) of C1q and 10 ng/ml (0.2 nM) of Wnt3A was comparable, as determined by *Axin2* mRNA induction (Figure 1L) and TOPFLASH reporter gene assay (Figure 4C), which indicates that 1,000 times more C1q molecules are required to activate Wnt signaling to the same extent that Wnt3A does. These apparent discrepancies may be explained by the unique mode of Wnt signaling activation by C1q compared to that by classical Wnt proteins. Activation of Wnt signaling by C1q requires several rate-limiting steps, which include the activation of C1q, C1r, and C1s. For instance, whether conformational change of C1q required for its activation occurs at the cell surface may be affected by the local density of Fz receptors, analogous to the mechanism of C1q activation by immunoglobulins (Duncan and Winter, 1988; Schumaker et al., 1986). This notion is consistent with our data showing that increasing the amount of Fz receptors potently decreased the EC_{50} value of C1q-induced activation of Wnt signaling (Figures 1M and 1N). Activation of C1r and C1s may be affected by their expression levels or by the local concentration of endogenous C1 inhibitor, which is also consistent with our observations that C1q-induced activation of Wnt signaling in skeletal muscle was observed only when the expressions of C1r and C1s were upregulated following injury (Figures 6C–6E) and that treatment with C1 inhibitor or knockdown of C1r/C1s reduced Wnt signaling activation by C1q (Figures 4B–4D and 5J). Thus, the extent of C1q-induced activation of Wnt signaling is highly context dependent and modulated not only by the concentration of C1q to which target cells are exposed, but also by many factors, including the expression levels of Fz receptors, LRP5/6 coreceptors, C1r, C1s, and C1 inhibitor in target cells.

LRP5/6 mutants lacking the extracellular domain have been reported to be a constitutively active form of canonical Wnt signaling (Liu et al., 2003; Mao et al., 2001). Our findings indicate that cleavage of extracellular N-terminal region of LRP5/6 by C1s occurs under physiological situations. Moreover, C1q treatment phosphorylated both cleaved and uncleaved LRP6, and overexpression of truncated LRP6 phosphorylated simultaneously overexpressed full-length LRP6 in the absence of ligand stimulation (Figures S3A–S3C), indicating that cleaved LRP5/6 fragment may amplify Wnt signaling by inducing the phosphorylation of

(C) X-gal staining of skeletal muscle after injury. Skeletal muscle of young (2 months old) TOPGAL mice was cryoinjured and treated with PBS or C1q (50 μg/ml). X-gal staining showed that β-gal activity was slightly increased 2 days after cryoinjury, which was enhanced by C1q.

(D) Quantitative analysis of β-gal activity. TOPGAL mice were treated as in (C), and tissue β-gal activity was measured and corrected with tissue weight. Data are presented as mean ±SD. *$p < 0.01$ versus sham-operated mice treated with PBS ($n = 10$).

(E) Real-time PCR analysis. Mice were treated as in (C), and the expressions of *Irp5*, *Irp6*, *C1r*, and *C1s* were analyzed by real-time PCR. Data are presented as mean ±SD. *$p < 0.01$ versus sham-operated mice ($n = 6$).

(F and G) BrdU incorporation assay in satellite cells (F) and fibroblasts (G). Satellite cells and fibroblasts were stimulated with C1q (100 μg/ml) or Wnt3A (10 ng/ml) for 24 hr. BrdU incorporation during the last 12 hr (satellite cells) or 4 hr (fibroblasts) was assayed by ELISA. C1q and Wnt3A inhibited satellite cell proliferation and stimulated fibroblast proliferation. Data are presented as mean ±SD. *$p < 0.01$ versus control ($n = 4$).

(H) Collagen concentration in the culture media. After stimulation with C1q (100 μg/ml) or Wnt3A (10 ng/ml) for 24 hr, medium was changed to serum-free medium, and soluble collagen released to the medium was quantified 6 hr later. C1q and Wnt3A increased collagen production in fibroblasts. Data are presented as mean ±SD. *$p < 0.01$ compared with control ($n = 4$).

(I and J) BrdU incorporation assay in satellite cells (I) and fibroblasts (J). Satellite cells and fibroblasts were cultured and stimulated with serum (5%) for 24 hr. BrdU incorporation was assayed as in (F) and (G). Serum from aged mice reduced satellite cell proliferation and stimulated fibroblast proliferation, which was attenuated by M241. Data are presented as mean ±SD. *$p < 0.01$ versus serum from young mice. **$p < 0.01$ versus serum from aged mice ($n = 4$).

(K) Collagen concentration in the culture media. After stimulation with serum for 24 hr, soluble collagen in the medium was assayed as in (H). Serum from aged mice increased collagen production in fibroblasts, which was attenuated by M241 treatment. *$p < 0.01$ versus serum from young mice. Data are presented as mean ±SD. **$p < 0.01$ versus serum from aged mice ($n = 4$).

(L and M) Number of proliferating satellite cells (L) and fibroblasts (M) in cryoinjured skeletal muscle of young mice (2 months old) in vivo. Sections were immunostained with M-cadherin (a satellite cell marker), Vimentin (a fibroblast marker), and phospho-histone H3 (pH3) (a mitotic marker). Proliferating satellite cells and fibroblasts were identified as M-cadherin/pH3 double-positive cells and Vimentin/pH3 double-positive cells, respectively. C1q treatment reduced satellite cell proliferation and stimulated fibroblast proliferation in cryoinjured skeletal muscle. Data are presented as mean ±SD. *$p < 0.05$ versus control ($n = 5$). See also Figure S4.

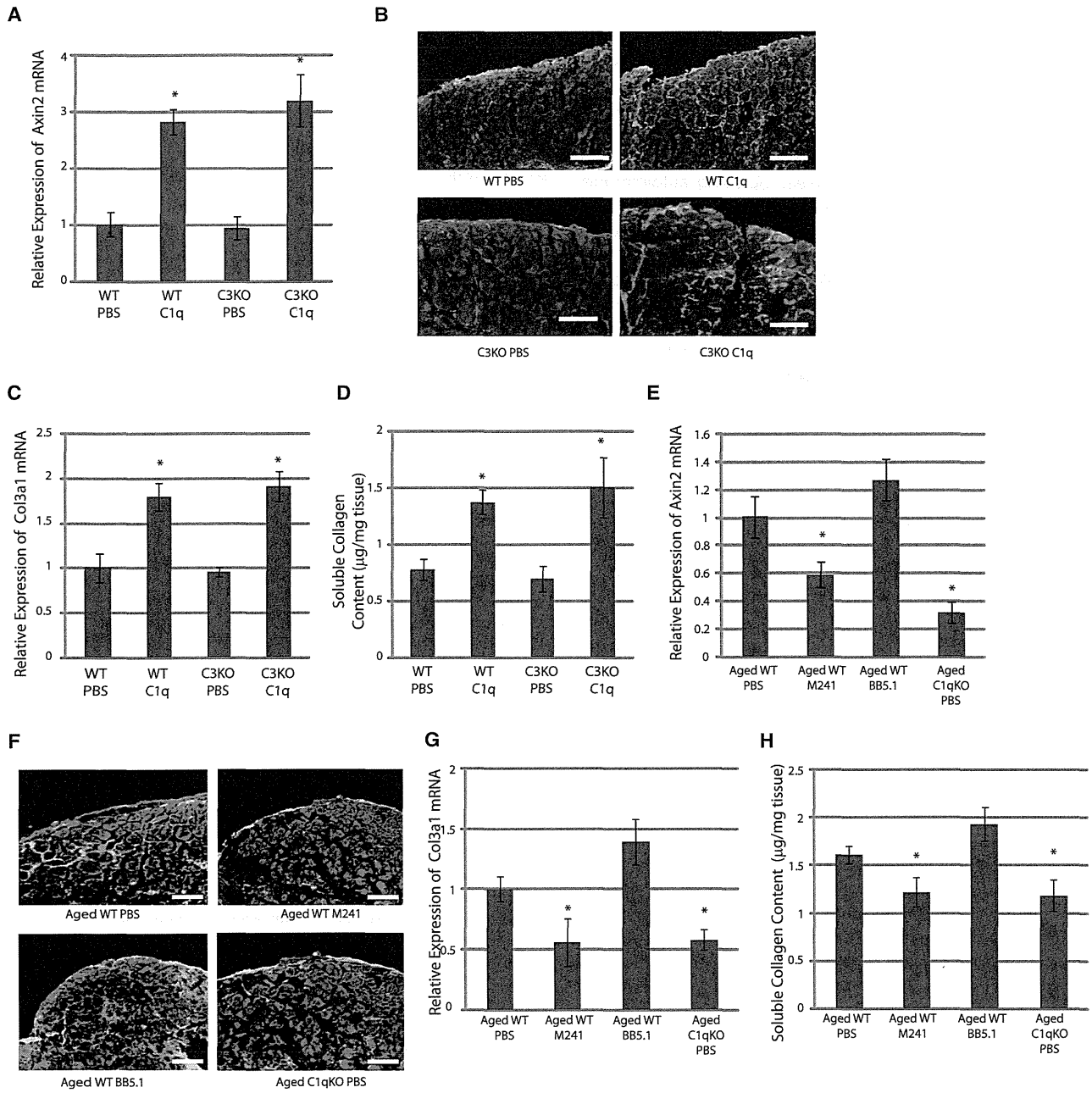

Figure 7. C1q Mediates Reduced Regenerative Capacity of Skeletal Muscle Associated with Aging

(A) *Axin2* mRNA expression. Skeletal muscle of young (2 months old) wild-type (WT) and C3-deficient (C3KO) mice was cryoinjured and treated with PBS or C1q (50 μg/ml). RNA was extracted 3 days later. C1q treatment increased *Axin2* gene expression in injured skeletal muscle of both wild-type and C3-deficient mice. Data are presented as mean ±SD. *$p < 0.01$ versus PBS ($n = 4$).

(B) Immunostaining of skeletal muscle after cryoinjury. Tissue samples were harvested 5 days after injury and immunostained with embryonic myosin heavy-chain (Red) and type I/III Collagen (green). Four wild-type mice (eight samples) and three C3-deficient mice (six samples) were used for each group, and representative figures are shown. C1q treatment impaired muscle regeneration and increased fibrosis in both wild-type and C3-deficient mice. Scale bar, 150 μm.

(C) Expression of *Col3a1* gene. RNA was harvested 3 days after injury. C1q treatment increased *Col3a1* expression in injured skeletal muscle of both wild-type and C3-deficient mice. Data are presented as mean ±SD. *$p < 0.01$ versus PBS ($n = 4$).

(D) Soluble collagen content in skeletal muscle. Samples were harvested 5 days after injury. C1q treatment increased soluble collagen content in skeletal muscle after cryoinjury of both wild-type and C3-deficient mice. Data are presented as mean ±SD. *$p < 0.01$ versus PBS ($n = 4$).

(E) *Axin2* mRNA expression. Skeletal muscle of aged (2 years old) wild-type (WT) mice or aged C1qa-deficient mice (C1qKO) was cryoinjured and treated with M241 or BB5.1 (500 μg/ml each). RNA was extracted 3 days after cryoinjury. The expression of *Axin2* was suppressed by M241 treatment or in C1qa-deficient mice, but not by BB5.1 treatment. Data are presented as mean ±SD. *$p < 0.01$ versus aged WT PBS ($n = 4$).

uncleaved LRP5/6. Although the precise mechanism by which full-length LRP5/6 is phosphorylated in the presence of cleaved form of LRP5/6 is currently unknown, these observations may, in part, explain the reason why cleavage of a small fraction of LRP5/6 by C1q treatment leads to activation of Wnt signaling to the comparable level induced by Wnt3A.

In addition to its role in innate immunity, C1q is implicated in the pathogenesis of various diseases, including autoimmunity and neurodegenerative diseases (Nayak et al., 2010). C1q deficiency in humans is tightly associated with the development of systemic lupus erythematosus (SLE) (Pickering et al., 2000), and it has been reported that Wnt/β-catenin signaling plays a role in the immune system by regulating T cell development and dendritic cell maturation (Manicassamy et al., 2010; Staal et al., 2008; Xu et al., 2003). It would be interesting to test whether downregulation of Wnt signaling activity in lymphocytes plays a role in the development of autoimmunity. In the central nervous system, complement system can be both protective and deleterious because it works to eliminate toxic proteins, whereas its sustained activation induces the production of cytokines or oxidative products from microglia (Bonifati and Kishore, 2007). C1q also mediates synapse elimination during development and is reactivated in the retina of mice with glaucoma (Stevens et al., 2007). Intriguingly, activation of Wnt signaling in the brain has also been reported to be both protective and deleterious (Boonen et al., 2009), and Wnt signaling has been shown to exert both positive and negative effects on synapse formation (Klassen and Shen, 2007; Packard et al., 2002). It remains elusive whether increased activation of canonical Wnt signaling by C1q contributes to aging-associated neurological disorders.

In summary, we have shown that complement C1q is an activator of canonical Wnt signaling and that activation of Wnt signaling by C1q mediates impaired regenerative capacity of skeletal muscle in aged animals. These findings suggest that C1q-induced activation of Wnt signaling plays an important role in other aging-related phenotypes as well as in the pathogenesis of various diseases that are related to augmented Wnt signaling. Likewise, impaired function of C1q may play a pathogenic role in the disease states associated with reduced Wnt signaling. Modulation of C1q-dependent activation of Wnt signaling may provide a therapeutic strategy for diseases linked to dysregulated Wnt signaling.

EXPERIMENTAL PROCEDURES

Cell Culture

HEK293, NIH 3T3, and HepG2 cells were cultured in DMEM containing 10% fetal bovine serum. Satellite cells in skeletal muscle were isolated as described (Brack et al., 2007). Fibroblasts in skeletal muscle were prepared by repeated digestion of skeletal muscle by trypsin.

TOPFLASH Assay

TOPFLASH assay was performed using a HEK293 cell line stably transfected with a luciferase reporter gene under the control of eight Tcf/Lef-binding sites (Super 8XTOPFLASH) (Veeman et al., 2003). Twenty-four hours after passage, cells were serum starved for 3 hr before stimulation. Luciferase assay was performed 24 hr after stimulation. Luciferase activity was determined using One-Glo (Promega), as described (Naito et al., 2006). Experiments were performed in triplicate for at least three different samples. Results are shown as the fold induction of the luciferase activity relative to the control.

β-Catenin Stabilization Assay

HEK293 or HepG2 cells were used for β-catenin stabilization assay. Twenty-four hours after passage, cells were serum starved for 24 hr before stimulation. At 1 hr after stimulation, cytosolic fraction was obtained by ultracentrifugation.

RNA Analysis

Relative levels of gene expression were quantified by the comparative Ct method using Universal Probe Library (UPL) (Roche) and Light Cycler TaqMan Master kit (Roche).

Protein Analysis

Total cell lysate was collected in lysis buffer containing 1% Triton X-100. Cytosolic and membrane/organelle fraction was obtained by differential centrifugation. Culture medium was concentrated using Amicon Ultra (Millipore) or immunoprecipitated with anti-myc antibody.

Binding Assays

C1q/Wnt3A was labeled with succinimidyl alkyne (Invitrogen), and various concentrations of labeled C1q/Wnt3A were mixed with 500 fmol (~21.65 ng) of Fz8/Fc in a volume of 100 μl (5 nM). C1q/Wnt3A that bound to Fz8/Fc was coprecipitated with protein G, eluted, quantified by ELISA using biotin-azide and HRP-streptavidin, and shown as the molar that binds specifically to 1 mg of Fz8/Fc. Unbound C1q/Wnt3A was collected and also quantified by ELISA.

Cell Proliferation Assay

Proliferation of cultured satellite cells and fibroblasts derived from skeletal muscle was assayed using Cell Proliferation ELISA, BrdU (Colorimetric) (Roche). Different durations of BrdU labeling time between satellite cells and fibroblasts are due to their difference in proliferative capacity.

Soluble Collagen Assay

Collagen content in culture media was assayed using Sircoll Collagen Assay (Biocolor). Tissue collagen content was assessed in the same manner after extraction of salt-soluble collagens using extraction buffer (50 mM Tris and 1.0 M NaCl plus protease inhibitors).

Animals

All protocols were approved by the Institutional Animal Care and Use Committee of Chiba University and Osaka University. TOPGAL mice were from Jackson laboratory. C1qa-deficient mice (Botto et al., 1998) and C3-deficient mice (Wessels et al., 1995) were previously described. Mice backcrossed to C57BL/6 background were used.

Statistical Analysis

Data are expressed as mean ±SD. The significance of differences among means was evaluated using analysis of variance (ANOVA), followed by

(F) Immunostaining of skeletal muscle after cryoinjury. Tissue samples were harvested 5 days after injury and immunostained as in (B). Three wild-type mice (six samples) and two C1qa-deficient mice (four samples) were used, and representative figures are shown. Impaired skeletal muscle regeneration in aged mice was restored by M241 treatment, but not by BB5.1 treatment, and was not observed in C1qa-deficient mice. Scale bar, 150 μm.

(G) Expression of *Col3a1* gene. RNA was extracted 3 days after cryoinjury. The expression of *Col3a1* gene was reduced by M241 treatment or in C1qa-deficient mice, but not by BB5.1 treatment. Data are presented as mean ±SD. *$p < 0.01$ versus aged WT PBS ($n = 4$).

(H) Soluble collagen content in skeletal muscle. Samples were harvested 5 days after cryoinjury. Soluble collagen content was attenuated by M241 treatment or in C1qa-deficient mice, but not by BB5.1 treatment. Data are presented as mean ±SD. *$p < 0.01$ versus aged WT PBS ($n = 6$).

Mann-Whitney's U test or Fisher's PLSD test for comparisons. Significant differences were defined as $p < 0.05$.

SUPPLEMENTAL INFORMATION

Supplemental Information includes Extended Experimental Procedures and four figures and can be found with this article online at doi:10.1016/j.cell.2012.03.047.

ACKNOWLEDGMENTS

We thank X. He, R.T. Moon, C. Niehrs, and S. Aizawa for plasmids and A. Furuyama, M. Iiyama, M. Ikeda, M. Kikuchi, M. Naito, Y. Ohtsuki, and I. Sakamoto for technical support. This work was supported by grants from the Ministry of Education, Culture, Sports, Science and Technology (MEXT); the Ministry of Health, Labour, and Welfare; and Japan Science and Technology Agency (to I.K.). This work was also supported by Grant-in-Aid for Young Scientists (A), Grant-in-Aid for JSPS Fellows, Research Grant from the Japan Prize Foundation, and the Japan Foundation for Applied Enzymology (to A.T.N.).

Received: March 8, 2010
Revised: November 13, 2010
Accepted: March 28, 2012
Published: June 7, 2012

REFERENCES

Ahn, V.E., Chu, M.L., Choi, H.J., Tran, D., Abo, A., and Weis, W.I. (2011). Structural basis of Wnt signaling inhibition by Dickkopf binding to LRP5/6. Dev. Cell *21*, 862–873.

Angers, S., and Moon, R.T. (2009). Proximal events in Wnt signal transduction. Nat. Rev. Mol. Cell Biol. *10*, 468–477.

Blanpain, C., Horsley, V., and Fuchs, E. (2007). Epithelial stem cells: turning over new leaves. Cell *128*, 445–458.

Bonifati, D.M., and Kishore, U. (2007). Role of complement in neurodegeneration and neuroinflammation. Mol. Immunol. *44*, 999–1010.

Boonen, R.A., van Tijn, P., and Zivkovic, D. (2009). Wnt signaling in Alzheimer's disease: up or down, that is the question. Ageing Res. Rev. *8*, 71–82.

Borque, L., Olivan, V., and Iguaz, F. (1995). Development and validation of an automated particle-enhanced nephelometric immunoassay method for the measurement of human plasma C1q. J. Clin. Lab. Anal. *9*, 302–307.

Botto, M., Dell'Agnola, C., Bygrave, A.E., Thompson, E.M., Cook, H.T., Petry, F., Loos, M., Pandolfi, P.P., and Walport, M.J. (1998). Homozygous C1q deficiency causes glomerulonephritis associated with multiple apoptotic bodies. Nat. Genet. *19*, 56–59.

Brack, A.S., Conboy, M.J., Roy, S., Lee, M., Kuo, C.J., Keller, C., and Rando, T.A. (2007). Increased Wnt signaling during aging alters muscle stem cell fate and increases fibrosis. Science *317*, 807–810.

Chen, S., Bubeck, D., MacDonald, B.T., Liang, W.X., Mao, J.H., Malinauskas, T., Llorca, O., Aricescu, A.R., Siebold, C., He, X., and Jones, E.Y. (2011). Structural and functional studies of LRP6 ectodomain reveal a platform for Wnt signaling. Dev. Cell *21*, 848–861.

Clevers, H. (2006). Wnt/beta-catenin signaling in development and disease. Cell *127*, 469–480.

Duncan, A.R., and Winter, G. (1988). The binding site for C1q on IgG. Nature *332*, 738–740.

Eriksson, H., and Nissen, M.H. (1990). Proteolysis of the heavy chain of major histocompatibility complex class I antigens by complement component C1s. Biochim. Biophys. Acta *1037*, 209–215.

Kang, Y.S., Do, Y., Lee, H.K., Park, S.H., Cheong, C., Lynch, R.M., Loeffler, J.M., Steinman, R.M., and Park, C.G. (2006). A dominant complement fixation pathway for pneumococcal polysaccharides initiated by SIGN-R1 interacting with C1q. Cell *125*, 47–58.

Kikuchi, A., Yamamoto, H., and Kishida, S. (2007). Multiplicity of the interactions of Wnt proteins and their receptors. Cell. Signal. *19*, 659–671.

Klassen, M.P., and Shen, K. (2007). Wnt signaling positions neuromuscular connectivity by inhibiting synapse formation in C. elegans. Cell *130*, 704–716.

Liu, G., Bafico, A., Harris, V.K., and Aaronson, S.A. (2003). A novel mechanism for Wnt activation of canonical signaling through the LRP6 receptor. Mol. Cell. Biol. *23*, 5825–5835.

Liu, H., Fergusson, M.M., Castilho, R.M., Liu, J., Cao, L., Chen, J., Malide, D., Rovira, I.I., Schimel, D., Kuo, C.J., et al. (2007). Augmented Wnt signaling in a mammalian model of accelerated aging. Science *317*, 803–806.

Logan, C.Y., and Nusse, R. (2004). The Wnt signaling pathway in development and disease. Annu. Rev. Cell Dev. Biol. *20*, 781–810.

MacDonald, B.T., Tamai, K., and He, X. (2009). Wnt/beta-catenin signaling: components, mechanisms, and diseases. Dev. Cell *17*, 9–26.

Manicassamy, S., Reizis, B., Ravindran, R., Nakaya, H., Salazar-Gonzalez, R.M., Wang, Y.C., and Pulendran, B. (2010). Activation of beta-catenin in dendritic cells regulates immunity versus tolerance in the intestine. Science *329*, 849–853.

Mao, B., Wu, W., Li, Y., Hoppe, D., Stannek, P., Glinka, A., and Niehrs, C. (2001). LDL-receptor-related protein 6 is a receptor for Dickkopf proteins. Nature *411*, 321–325.

Matsumoto, M., and Nagaki, K. (1986). Functional analysis of activated C1s, a subcomponent of the first component of human complement, by monoclonal antibodies. J. Immunol. *137*, 2907–2912.

Naito, A.T., Shiojima, I., Akazawa, H., Hidaka, K., Morisaki, T., Kikuchi, A., and Komuro, I. (2006). Developmental stage-specific biphasic roles of Wnt/beta-catenin signaling in cardiomyogenesis and hematopoiesis. Proc. Natl. Acad. Sci. USA *103*, 19812–19817.

Nayak, A., Ferluga, J., Tsolaki, A.G., and Kishore, U. (2010). The non-classical functions of the classical complement pathway recognition subcomponent C1q. Immunol. Lett. *131*, 139–150.

Packard, M., Koo, E.S., Gorczyca, M., Sharpe, J., Cumberledge, S., and Budnik, V. (2002). The Drosophila Wnt, wingless, provides an essential signal for pre- and postsynaptic differentiation. Cell *111*, 319–330.

Petry, F., Botto, M., Holtappels, R., Walport, M.J., and Loos, M. (2001). Reconstitution of the complement function in C1q-deficient (C1qa-/-) mice with wild-type bone marrow cells. J. Immunol. *167*, 4033–4037.

Pickering, M.C., Botto, M., Taylor, P.R., Lachmann, P.J., and Walport, M.J. (2000). Systemic lupus erythematosus, complement deficiency, and apoptosis. Adv. Immunol. *76*, 227–324.

Schumaker, V.N., Hanson, D.C., Kilchherr, E., Phillips, M.L., and Poon, P.H. (1986). A molecular mechanism for the activation of the first component of complement by immune complexes. Mol. Immunol. *23*, 557–565.

Staal, F.J., Luis, T.C., and Tiemessen, M.M. (2008). WNT signalling in the immune system: WNT is spreading its wings. Nat. Rev. Immunol. *8*, 581–593.

Stevens, B., Allen, N.J., Vazquez, L.E., Howell, G.R., Christopherson, K.S., Nouri, N., Micheva, K.D., Mehalow, A.K., Huberman, A.D., Stafford, B., et al. (2007). The classical complement cascade mediates CNS synapse elimination. Cell *131*, 1164–1178.

Tamai, K., Zeng, X., Liu, C., Zhang, X., Harada, Y., Chang, Z., and He, X. (2004). A mechanism for Wnt coreceptor activation. Mol. Cell *13*, 149–156.

Veeman, M.T., Slusarski, D.C., Kaykas, A., Louie, S.H., and Moon, R.T. (2003). Zebrafish prickle, a modulator of noncanonical Wnt/Fz signaling, regulates gastrulation movements. Curr. Biol. *13*, 680–685.

Walport, M.J. (2001). Complement. First of two parts. N. Engl. J. Med. *344*, 1058–1066.

Wessels, M.R., Butko, P., Ma, M., Warren, H.B., Lage, A.L., and Carroll, M.C. (1995). Studies of group B streptococcal infection in mice deficient in complement component C3 or C4 demonstrate an essential role for complement in both innate and acquired immunity. Proc. Natl. Acad. Sci. USA *92*, 11490–11494.

White, B.D., Nguyen, N.K., and Moon, R.T. (2007). Wnt signaling: it gets more humorous with age. Curr. Biol. *17*, R923–R925.

Xu, Y., Banerjee, D., Huelsken, J., Birchmeier, W., and Sen, J.M. (2003). Deletion of beta-catenin impairs T cell development. Nat. Immunol. *4*, 1177–1182.

Yamamoto, A., Nagano, T., Takehara, S., Hibi, M., and Aizawa, S. (2005). Shisa promotes head formation through the inhibition of receptor protein maturation for the caudalizing factors, Wnt and FGF. Cell *120*, 223–235.

Yonemasu, K., Kitajima, H., Tanabe, S., Ochi, T., and Shinkai, H. (1978). Effect of age on C1q and C3 levels in human serum and their presence in colostrum. Immunology *35*, 523–530.

Zeng, X., Tamai, K., Doble, B., Li, S., Huang, H., Habas, R., Okamura, H., Woodgett, J., and He, X. (2005). A dual-kinase mechanism for Wnt co-receptor phosphorylation and activation. Nature *438*, 873–877.

Zeng, X., Huang, H., Tamai, K., Zhang, X., Harada, Y., Yokota, C., Almeida, K., Wang, J., Doble, B., Woodgett, J., et al. (2008). Initiation of Wnt signaling: control of Wnt coreceptor Lrp6 phosphorylation/activation via frizzled, dishevelled and axin functions. Development *135*, 367–375.

Cardiovasc Drugs Ther (2012) 26:409–416
DOI 10.1007/s10557-012-6410-4

Design and Rationale of Low-Dose Erythropoietin in Patients with ST-Segment Elevation Myocardial Infarction (EPO-AMI-II Study): A Randomized Controlled Clinical Trial

Tetsuo Minamino · Ken Toba · Shuichiro Higo · Daisaku Nakatani · Shungo Hikoso · Masao Umegaki · Kouji Yamamoto · Yoshiki Sawa · Yoshifusa Aizawa · Issei Komuro · EPO-AMI-II study investigators

Published online: 2 September 2012

Abstract
Purpose The development of novel pharmaceutical interventions to improve the clinical outcomes of patients with acute ST-segment elevation myocardial infarction (STEMI) is an unmet medical need worldwide. In animal models, a single intravenous administration of erythropoietin (EPO) during reperfusion improves left ventricular (LV) function in the chronic stage. However, the results of recent proof-of-concept trials using high-dose EPO in patients with STEMI are inconsistent. In our pilot study, low-dose EPO after successful percutaneous coronary intervention (PCI) improved the LV ejection fraction (EF) and did not trigger severe adverse clinical events in patients with STEMI. One possible reason for this discrepancy is the dose of EPO used.
Methods and results We have started a double-blind, placebo-controlled, randomized, multicenter clinical trial (EPO-AMI-II) to clarify the safety and efficacy of low-dose EPO in patients with STEMI. STEMI patients who have a low LVEF (<50 %) will be randomly assigned to intravenous administration of placebo or EPO (6,000 or 12,000 IU) within 6 h after successful PCI. The primary endpoint is the difference in LVEF between the acute and chronic phases (6 months), as measured by single-photon emission computed tomography. The patient number needed for EPO-AMI-II is 600. The study will stop when superior efficacy or futility is detected by an interim analysis. This study has been approved by the Evaluation System of Investigational Medical Care.
Conclusions EPO-AMI-II study will clarify the safety and efficacy of low-dose EPO in STEMI patients with LV dysfunction in a double-blind, placebo-controlled, multicenter study. (247 words)

Key words Erythropoietin · Low-dose · Acute myocardial infarction · LV dysfunction

Names of Grants: Grants-in-Aid from the Ministry of Health, Labour and Welfare (Japan); the Ministry of Education's Support and Training Program for Translational Research at Osaka University; and the Japanese Circulation Society Grant for Translational Research 2010

T. Minamino · S. Higo · D. Nakatani · S. Hikoso · Y. Sawa · I. Komuro (✉)
Department of Cardiovascular Medicine,
Osaka University Graduate School of Medicine,
2-2 Yamada-oka,
Suita, Osaka 565-0871, Japan
e-mail: komuro-tky@umin.ac.jp

K. Yamamoto
Department of Biomedical Statistics,
Osaka University Hospital,
Suita, Japan

M. Umegaki
Medical Center for Translational Research, Osaka University Hospital,
Suita, Japan

K. Toba
First Department of Internal Medicine,
Niigata University Medical and Dental Hospital,
Niigata, Japan

Y. Aizawa
Tachikawa Medical Center,
Nagaoka, Japan

Despite improved clinical outcomes by early reperfusion with thrombolysis and primary percutaneous coronary intervention (PCI) with stenting, the mortality of patients with

ST-segment elevation myocardial infarction (STEMI) is still high in Western countries and Japan [1, 2]. Furthermore, in the chronic stage after MI, heart failure can develop due to left ventricular (LV) remodeling [3]. To date, most clinically tested agents that induce cardioprotection have failed to reduce infarct size in clinical settings [4]. Thus, novel pharmaceutical interventions to improve the clinical outcomes of patients with STEMI are urgently needed. Animal studies show that the intravenous administration of erythropoietin (EPO), a glycoprotein hormone consisting of 165 amino acid residues [5], at the onset of reperfusion reduces the myocardial infarct size and prevents cardiac remodeling, with enhanced neovascularization in the heart after MI [6, 7]. Several proof-of-concept studies have been performed to clarify the cardioprotective effects of EPO in patients with STEMI. The administration of high-dose EPO (60,000–99,000 IU) did not improve left ventricular ejection fraction (LVEF) or reduce infarct size [8–10]. Regarding secondary endpoints, the use of EPO has been associated with a trend toward an increase in major adverse cardiovascular events in 2 studies [8, 10] and significantly fewer events in a third study [9]. In contrast, low-dose EPO is likely to be cardioprotective, according to small clinical trials [11–13]. Platelet activation by high-dose EPO [14] and the existence of an optimal dose for limiting infarct size [15] may explain the dose-dependent discrepancy of EPO-induced cardioprotection. Importantly, pilot studies showed that low-dose EPO is associated with improved left ventricular function without major adverse cardiovascular events [11, 12]. Furthermore, our post-hoc analysis revealed that EPO administration was highly associated with improved LV function in STEMI patients with a low LV ejection fraction (LVEF) (<50 %) (Fig. 1). Therefore, we have started a double-blind, placebo-controlled, randomized, multicenter clinical trial (EPO-AMI-II) to clarify the safety and efficacy of low-dose EPO in STEMI patients with a low LVEF (<50 %). The protocol was submitted to the Evaluation System of Investigational Medical Care of the Ministry of Health, Labour and Welfare of Japan and was approved under the Japanese governmental health insurance system on 1 August 2011.

Methods

Study objects

The objectives of this study are to evaluate whether a single bolus administration of EPO prevents ischemia-reperfusion injury dose-dependently and to estimate the optimum clinical dose of EPO in patients with STEMI after successful PCI by analyzing the improvement in LVEF between the acute and chronic stages.

Study design

EPO-AMI-II is an ongoing multicenter, prospective, randomized, double-blind, placebo-controlled, dose-finding study in patients presenting with a first STEMI. After a successful PCI, patients will be randomly assigned to receive either an intravenous bolus dose of epoetin-beta (EPO) (6,000 or 12,000 IU) or placebo on top of standard medical care (Fig. 2). This trial was registered at the UMIN Clinical Trials Registry as UMIN000005721.

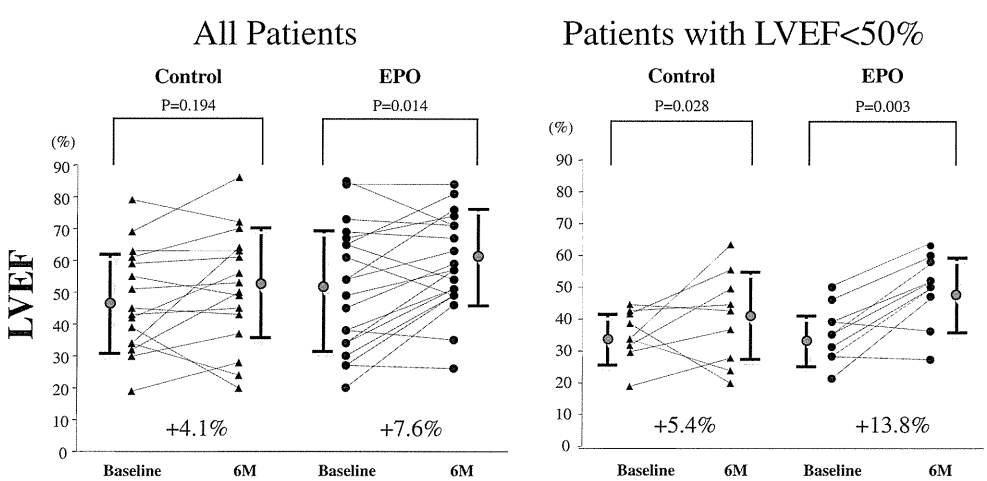

Fig. 1 Post-hoc analysis of the EPO-AMI-I results. Panel **a** shows the LVEF between the acute and chronic stages in all patients in the EPO-AMI-I study. EPO, but not saline, administration significantly increased LVEF at 6 months after an MI. Panel **b** shows the LVEF between the acute and chronic stages in patients with LVEF <50 % in the EPO-AMI-I study. Both saline and EPO significantly increased LVEF at 6 months after an MI. The improvement of LVEF did not significantly differ between the saline- and EPO-treated groups. See the abbreviation definitions in the text

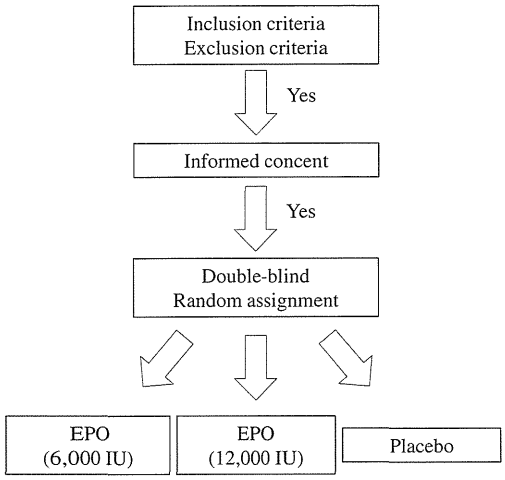

Fig. 2 Study flow chart

Patients

Consecutive patients with diagnostic signs and symptoms of an acute MI who satisfy the study inclusion and exclusion criteria (Table 1). After successful PCI, patients will be asked for written informed consent, and if they agree, will be assigned according to a pre-defined central web-based randomization system to receive EPO or placebo on top of optimal standard medical care. Patients will receive the study drug within 6 h after PCI. The patient, the attending physician, and the staff performing SPECT and the clinical follow-up will be unaware of the assigned treatment.

End points

The primary end point of this study is to evaluate the LVEF improvement between the acute (days 4–7) and chronic stages (6 months) (Table 2). The secondary end points of this study are to evaluate the efficacy and safety of EPO treatment. The efficacy is evaluated by analyzing indices of cardiac function 6 months after EPO administration. These are calculated with electrocardiogram-gated single-photon emission computed tomography (SPECT) and include LV end-diastolic volume (LVEDV), LV end-systolic volume (LVESD), LVEDV index, LVESV index, regional wall motion score, % uptake at resting, and defect size. The survival ratio, cardiovascular events (defined as cardiac death, stroke, nonlethal myocardial infarction, admission due to worsening of heart failure or unstable angina, revascularization, and onset of heart failure symptoms), and NT-ProBNP at the 6-month follow-up will also be analyzed to evaluate the efficacy of EPO treatment (Table 2). The safety is based on the incidence of major adverse events, clinical laboratory test data and vital signs.

Table 1 Inclusion and exclusion criteria

Inclusion criteria
1. Patients with first-time myocardial infarction
2. Patients with ST-elevation acute myocardial infarction (AMI) who have successful reperfusion by PCI within 12 h after the symptom onset
3. Patients whose ejection fraction at enrollment is <50 % on UCG or LVG
4. Age: over 20 years old, under 80 years old
5. Patients who agreed with participation to the trial in writing
Exclusion critetia
1. Patients with significant stenotic lesions in non infarct-related artery which require revascularization
2. Patients who resulted in obviously impaired reperfusion
3. Patients with Killip class III or IV, or cardiogenic shock at admission
4. Patients with advanced renal or hepatic dysfunction (Cre more than 2 mg/dl, or T-Bil more than 3 mg/dl)
5. Patients with blood pressure more than 140/90 mmHg after PCI
6. Hematocrit more than 54 % on admission
7. Patients who exhibit atrial fibrillation after PCI
8. Patients who have been diagnosed with malignant hypertension
9. Patients who have previously received treatment with EPO
10. Patients who received a blood transfusion in the last 3 months
11. Patients who are or have been diagnosed with cancer in the past 5 years
12. Patients who are complicated with severe infection such as pneumonia or sepsis
13. Patients who are contraindicated to aspirin or thienopyridine derivatives
14. Women who are pregnant, breastfeeding, or have a possibility for pregnancy
15. Patients whom researchers judged that they are not appropriate to participate this trial

Study drug administration

Prior to or at the time of primary PCI, standard antithrombotic treatments for acute MI are administered. Within 6 h after PCI, the enrolled patients are randomly assigned to placebo or an Epo dose (6,000 or 12,000 IU). Active drug or placebo is diluted in 10 mL of saline and administered intravenously over 1 min. The double-blind administration is ensured by a subject identification code unknown to physicians, nurses and patients. Drug or placebo is prepared under medical supervision according to instructions contained in predefined packages provided by the EPO-AMI-II organization. Standard treatment, including beta-blockade, lipid-lowering therapy, and angiotensin-converting enzyme inhibition or angiotensin-II receptor blockade, is additionally prescribed. EPO and placebo are kind gifts of Chugai Pharmaceutical Co. Ltd (Tokyo, Japan).

Table 2 Primary and secondary end points

Primary end point
The improvement of left ventricular ejection fraction at the chronic phase (the mean of differences between LVEF value at 4–7 days and that at 6 months after administration)
Secondary end point
[Efficacy]
1. Indexes of cardiac function 6 months after administration of epoetin-beta, which are calculated with cardiac scintigraphy (LVEDV, LVESV, LVEDVI, LVESVI, regional wall motion score, ischemia and defect size (SRS (Summed rest Score), SDS (Summed difference Score), %Defect Size, %uptake at resting))
2. Survival ratio
3. Cardiac event ratio (Cardiac death, stroke, nonlethal myocardial infarction, admission due to worsening of heart failure or unstable angina, revasculization, onset of heart failure symptoms (typical dyspnea at rest or during exercise, pulmonary congestion or pretibial edema)
4. NT-ProBNP 6 months after administration
[safety]
1. Adverse events
2. Laboratory test data
3. Vital signs (blood pressure, pulse rate)

Clinical and laboratory measures

Blood pressure, heart rate, and ECG are monitored at regular intervals until discharge (Fig. 3). Major adverse events (as defined above) are recorded during hospitalization and up to 6 months thereafter. At 4–7 days after admission and at 6 months, cardiac SPECT is also performed to evaluate cardiac function.

Quantification of LV function and infarct size

We will perform ECG-gated 99mTc-MIBI SPECT 4–7 days after PCI as the baseline measurement and at the 6-month follow-up. The 99mTc-MIBI (600–740 MBq) is administered at baseline and at the 6-month follow-up. SPECT image acquisition is performed 60 min after the 99mTc-MIBI injection. ECG-gated SPECT is performed after the administration of 99mTc-MIBI at rest. In ECG gating, SPECT data divided into 16 equal intervals are analyzed using Quantitative Gated SPECT software (Cedars-Sinai Medical Center, Los Angeles, CA, USA), which is also used to calculate EDVI, ESVI and LVEF. Pharmacologic stress tests are performed with non-gated 99mTc-MIBI SPECT. Adenosine (Adenoscan; DAIICHI SANKYO, Tokyo, Japan) is administered at a rate of 0.72 mg/kg for 6 min. The 99mTc-MIBI is injected 3 min after the start of adenosine infusion. The non-gated SPECT image is used to assess the severity of myocardial perfusion abnormalities, and regional uptake and the infarct area are calculated using Quantitative Perfusion SPECT software (Cedars-Sinai Medical Center). Regional uptake is assessed by applying a 17-segment model of the left ventricle according to the standard myocardial segmentation of the Cardiac Imaging Committee of the Council on Clinical Cardiology of the American Heart Association. Regional uptake is expressed as the mean uptake count in these segments. Defects at less than the threshold of 60 % of peak counts are identified as infarcted myocardium, and the infarct area is expressed as a percentage of the entire left ventricle involved. SPECT data will be analyzed in a blinded fashion by the SPECT Core Center members with the assistant of nuclear medicine special radiological technologist at MICRON Co., Ltd (Molecular Imaging CRO Network, Tokyo, Japan.). Finally, the analyzed data will be evaluated by an independent RI assessment committee.

Adverse events and additional safety assessments

An independent data safety monitoring board (DSMB) will receive real-time clinical information and will perform interim safety and efficacy analyses at 33 %, 66 % and 100 % recruitment. There are no formal (statistical) rules for stopping treatment due to safety reasons in this study. The DSMB recommendations are based on a clinical assessment of the frequency, and the nature of the serious adverse events and their relation to the investigational treatment.

Sample size calculation

Based on the results of our pilot study in STEMI patients with LVEF <50 % (LVEF improvement in the EPO-II group: 13.80±9.85 %, n=11, and in the placebo group: 5.44±14.80 %, n=9) (Fig. 1), the difference in LVEF improvement between the EPO (12,000 IU) treatment group and the placebo group is estimated to be 4.42 % with a common standard deviation of 14.33 %. As a result, the effect size is estimated to be 0.31 [16]. To demonstrate the

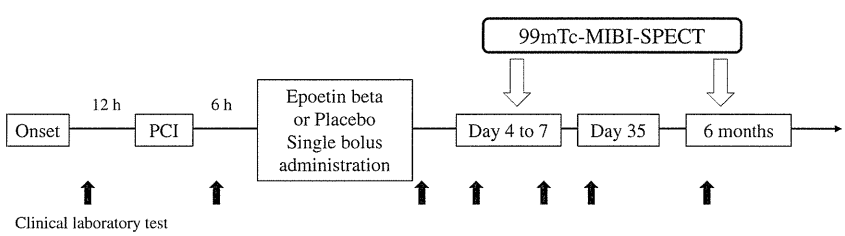

Fig. 3 Study schedule

treatment difference with a power of 0.85 and a 1-sided alpha of 0.025, 190 patients per group will be needed. However, because we plan to perform two interim analyses, we will need 193 patients per group [17]. Taking into account several patients dropping out, the total sample size to be recruited will be 200 patients in each treatment group, i.e., 600 patients will be recruited in this study.

Interim analysis

There will be two formal interim analyses on the safety and efficacy of the primary end point: after 198 and 396 randomized patients are enrolled and followed up for 6 months. For the interim analyses on efficacy, the DSMB will evaluate the primary end point using the Lan-DeMets method with the O'Brien-Fleming spending function. Asymmetric stopping boundaries are planned, with early termination of the study recommended in the event of evidence of overwhelming benefit (2-sided $P<.001$ favoring EPO) or substantive harm (2-sided $P<.01$ against EPO) once sufficient events have accrued.

Statistical analysis

Data will be analyzed based on an intention-to-treat principle. The efficacy end point is LVEF improvement. The null hypothesis, that all treatment groups will have the same mean LVEF improvement, will be tested against the alternative hypothesis, that the mean LVEF improvement in the treatment groups will increase in the order of placebo, EPO (6,000 IU) and EPO (12,000 IU), according to the contrast test with a contrast coefficient (−1, 0, 1) based on the t-statistic. The contrast test will be evaluated based on a 1-sided significance level of 0.025. The secondary efficacy end point of OS in each group will be analyzed by the Kaplan-Meier method and compared using the log-rank test. Cardiovascular events and NT-ProBNP at the 6-months follow-up will be analyzed by a nonparametric test (e.g., Wilcoxon rank sum test). Safety analyses will be performed to summarize the adverse events in each treatment group. The baseline characteristics of the study patients will be summarized using frequencies and percentages for categorical variables and using means with standard deviations for continuous variables.

Current status

EPO-AMI-II began enrolling patients in December 2011. As of May 15, 2012, the application for the Evaluation System of Investigational Medical Care is ongoing, and 14 of 24 eligible centers have been approved. Completion of study enrollment is targeted for September 30, 2014. Allowing for the 6-month follow-up of the final randomized patient, trial completion is anticipated by March 2015.

Discussion

We have started the EPO-AMI-II study to clarify the safety and efficacy of low-dose EPO in the improvement of LVEF in STEMI patients with a low LVEF (<50 %). EPO-AMI-II is a multicenter, prospective, randomized, double-blind, placebo-controlled, dose-finding study in patients with their first STEMI.

Randomized clinical studies to clarify the effects of low-dose EPO in patients with STEMI

Therapies that can reduce myocardial damage and augment neovascularization in the heart after an MI may be beneficial in patients with STEMI. Experimental studies demonstrate that the intravenous administration of EPO at the onset of reperfusion reduces myocardial infarct size and prevents cardiac reverse remodeling, with enhanced neovascularization in the heart after an MI [6, 7]. Recently, proof-of-concept studies using high-dose EPO have reported inconsistent cardioprotection results from EPO in patients with STEMI (Table 3). The use of high-dose EPO at the time of reperfusion for an acute MI to salvage the myocardium or to improve LV function will not be further pursued in any newly initiated study.

In contrast, low-dose EPO is likely to be cardioprotective in small clinical trials [11–13]. Potential mechanisms to explain the dose-dependent discrepancy of EPO in cardioprotection may be attributable to platelet activation and the existence of an optimal dose for limiting infarct size. Platelet activation by a high dose of EPO [14] and the existence of an optimal dose for limiting infarct size [15] may explain the dose-dependent discrepancy of EPO-induced cardioprotection. Because EPO has structural similarity with thrombopoietin, high-dose EPO increases platelet production and reactivity, which leads to an increased risk of thrombosis and cardiovascular events. Additionally, a dose response curve of the bioactivity of cytokines does not necessarily appear to be guided by a sigmoid function. Positive intracellular signal of cytokine receptors via serial chain reaction of protein tyrosine kinases is typically interfered by automated circuit reaction of protein tyrosine phosphatase such as SHP1 to avoid overdoing of growth and inflammation [18]. In fact, administration of high-dose EPO lost its cardioprotective activity in rat and mouse coronary ischemia/reperfusion models [15, 19]. The rationale for EPO treatment for

Table 3 Overview of randomized controlled studies investigating the effects of EPO in patients with acute myocardial infarction

Trial	Dose of EPO	Primary outcome	Result	Cardiovascular event
REVIVAL-3	33,333 IU×3 (0, 24, 48 h)	LV EF	No change	Increase (not significant)
HEBE-III	60,000 IU	Infarction size	No change	Decrease (significant)
REVEAL	60,000 IU	Infarction size	No change	Increase (not significant)
EPOC-AMI	6,000 IU×3 (day 0, 2, 4)	LV EF	Improve	No change
EPO-AMI-I	12,000 IU	LV EF	Improve	No change
EPO-AMI-II	6,000 or 12,000 IU	LV EF		

patients with STEMI lies in the low-dose EPO trials, although these have only been small clinical trials to date.

Protocol of EPO-AMI-II study

On the basis of a post-hoc analysis of our pilot study (EPO-AMI-I) and a recent proposal from workshops [20–22], we have modified the protocol for the EPO-AMI-II study. First, we created new inclusion criteria to include patients with an LVEF <50 %. Only patients who have large myocardial infarcts can receive benefits from any adjunctive therapy [23, 24]. Consistently, the post-hoc analysis of the EPO-AMI-I study revealed that STEMI patients with an LVEF <50 % received large benefits from EPO administration11 (Fig. 1). When patients with significant stenotic lesions in non-infarct-related arteries that required revascularization were excluded, more than 90 % of STEMI patients who met the inclusion and exclusion criteria presented with a proximal left anterior descending artery in the EPO-AMI-I study. This type of STEMI patient will receive more benefit from adjunctive therapy [23, 24]. Second, we have shortened the therapeutic time window from the onset of chest pain to reperfusion time (from 24 h to 12 h), which will also result in a shorter time window between EPO administration and the onset of chest pain. For example, in rats with a permanent coronary occlusion, EPO does not effectively reduce myocardial infarct size when administered ≥24 h after the MI [25]. These protocol modifications of the EPO-AMI-I study will improve the efficacy and safety of low-dose EPO in patients with STEMI.

Safety of EPO in STEMI patients

In the EPO-AMI-I (12,000 IU) and EPOC studies (6,000 IU × 3) in which low-dose EPO was administered, the risk of cardiovascular events was not increased [11, 12]. When high-dose EPO was administered, the results were inconsistent. In the REVEAL study, the subanalysis showed that EPO (60,000 IU) had a higher incidence of serious adverse events, although the authors noted that the analysis was based on a very small number of events. Conversely, in the HEBEIII study, the subanalysis revealed that EPO showed a trend toward a reduction of enzymatic infarct size and significantly reduced the incidence of the combined endpoint (cardiovascular death, myocardial infarction, in-stent thrombosis, unstable angina and heart failure). In the REVIVAL study, EPO (33,000 IU × 3) showed a trend toward an increased rate of serious adverse effects. Their meta-analysis showed that the administration of EPO appeared to be safe for patients with acute STEMI [26]. For the safety of patients in the EPO-AMI-II study, a report system for serious adverse events has been established, and the clinical research coordinator will often visit the hospitals that participate in this study. Recently, the post-hoc analysis suggested the association of high-dose EPO with the restenosis of the culprit lesion, although no significant differences in late lumen loss between the EPO and placebo groups were observed [27, 28]. Additionally, no significant difference in late lumen loss was found when low-dose EPO was used [11, 12].

Quantification of LV function and infarct size

In the EPO-AMI-II study, we are only including patients with a first STEMI because ECG-gated SPECT allows for no distinction between previous and new infarcts. The primary end point of this study is to evaluate the improvement of LVEF between the acute and chronic stages (Table 2). In the chronic stage, ECG-gated SPECT with adenosine allows for the evaluation of the residual myocardial ischemia. One alternative evaluation method is cardiac magnetic resonance imaging, which may be able to assess the at-risk area and the final infarct size, but this technique remains to be validated for quantification [29].

Conclusions

Because the randomized control trials conducted to date have used high-dose EPO and demonstrated heterogeneous results, the EPO-AMI-II study will clarify the safety and efficacy of low-dose EPO in STEMI patients with LV dysfunction in double-blind, placebo-controlled, multicenter studies (Appendix).

Acknowledgments We sincerely thank Drs. Akira Myoi and Yasutaka Hayashida (Medical Center for Translational Research Osaka University Hospital) and Dr. Yoichi Yamamoto (Center for Clinical Investigation and Research, Osaka University Hospital) for advice on conducting the EPO-AMI-II study. We also thank Dr. Hiroyuki Uesaka for statistical aspects of the study design. We thank Hiromi Umezome, Sakiko Ichijo (Center for Clinical Investigation and Research, Osaka University Hospital) for their assistants and Sugako Mitsuoka for her excellent secretarial work. The management of this study is supported by Grants-in-Aid from the Ministry of Health, Labour and Welfare of Japan, a Japanese Circulation Society Grant for Translational Research 2010 and the Support and Training Program for Translational Research at Osaka University.

Discloures None.

Appendix

Principle Investigators:

Aizawa Y, Komuro I.

Steering Committee:

Higo S, Ito H, Kato K, Kobayashi N, Ozawa T, Minamino T, Suzuki H. Tobaru T, Toba K.

Data Management:

Higo S, Takahara S (Medical Center for Translational Research Osaka University Hospital, Suita, Japan)

Statistical Analysis:

Yamamoto K, Hamasaki T (Department of Biomedical Statistics, Osaka University Graduate School of Medicine, Suita, Japan)

SPECT Core Center:

Ishida Y (Kansai Rosai Hospital Cardiovascular Center, Amagasaki, Japan), Sakata Y, (Department of Cardiovascular Medicine, Osaka University Graduate School of Medicine, Suita, Japan), Yoshimura N (Department of Radiology, Niigata University Medical and Dental Hospital, Niigata, Japan)

Data and Safety Monitoring Board:

Fujio Y (Laboratory of Clinical Science and Biomedicine, Graduate School of Pharmaceutical Sciences, Osaka University, Japan), Hasegawa S (Department of Cardiology, Osaka Kosei Nenkin Hospital, Osaka, Japan), Seki Y (Department of Internal Medicine (Hematology), Niigata Prefectural Shibata Hospital, Japan). Sugimoto T (Department of Mathematical Sciences, Hirosaki University Graduate School of Science and Technology, Japan)

EPO-AMI-II Investigators:

Chiba-Nishi General Hospital, Chiba, Japan.
Yoshida T, Kuramochi M
Dokkyo University School of Medicine, Tochigi, Japan;
Ishimitsu T, Kobayashi N
Fujisawa City Hospital, Fujisawa, Japan
Yano H, Himeno H
Higashi-Osaka City General Hospital, Osaka, Japan
Kijima Y, Ichikawa M
Kansai Rosai Hospital, Amagasaki, Japan;
Uematsu M, Watanabe T
Kanto Rosai Hospital, Kawasaki, Japan
Namiki A, Shibata M
Kokura Memorial Hospital, Kitakyushu, Japan
Yokoi H, Nomura A
National Cerebral and Cardiovascular Center, Suita, Japan
Yasuda S, Kotani J
Niigata University Medical and Dental Hospital, Niigata, Japan;
Toba K, Ozawa T
Nippon Medical School, Tokyo, Japan
Mizuno K, Yasutake M
Nozaki Tokushukai Hospital, Osaka, Japan
Okutsu M, Sumitsuji S
Okayama University Graduate School of Medicine, Dentistry and Pharmaceutical Sciences, Okayama, Japan;
Ito H, Kusano K
Osaka General Medical Center, Osaka, Japan;
Fukunami M, Yamada T
Osaka National Hospital, Osaka, Japan;
Yasumura Y, Hirooka K
Osaka Police Hospital, Osaka, Japan;
Ueda Y, Hirata A
Osaka Rosai Hospital, Sakai, Osaka, Japan;
Nishino M, Makino N
Osaka University Graduate School of Medicine, Suita, Japan;
Komuro I, Minamino T
Sakakibara Heart Institute, Fuchu, Japan
Tobaru T, Asano R
Senri Critical Care Medical Center, Osaka Saiseikai Senri Hospital, Suita, Japan
Ito N, Doi, Y
Shonan Kamakura General Hospital, Kamakura, Japan
Saito S, Tobita K
Showa University Fujigaoka Hospital, Yokohama, Japan;
Suzuki H, Wakabayashi K
Showa University School of Medicine, Tokyo, Japan
Kobayashi Y, Koba S
St. Marianna University School of Medicine, Kawasaki, Japan
Yoneyama Y, Akashi Y
Tachikawa General Hospital, Nagaoka, Niigata, Japan;
Aizawa Y, Sato M

References

1. Lloyd-Jones D, Adams RJ, Brown TM, et al. Executive summary: heart disease and stroke statistics–2010 update: a report from the American Heart Association. Circulation. 2010;121:948–54.

2. Takii T, Yasuda S, Takahashi J, et al. Trends in acute myocardial infarction incidence and mortality over 30 years in Japan: report from the MIYAGI-AMI Registry Study. Circ J. 2010;74:93–100.
3. Sutton MG, Sharpe N. Left ventricular remodeling after myocardial infarction: pathophysiology and therapy. Circulation. 2000;101:2981–8.
4. Minamino T. Cardioprotection from ischemia/reperfusion injury: basic and translational research. Circ J. 2012;76:1074–82.
5. Jelkmann W. Erythropoietin: structure, control of production, and function. Physiol Rev. 1992;72:449–89.
6. Hirata A, Minamino T, Asanuma H, et al. Erythropoietin just before reperfusion reduces both lethal arrhythmias and infarct size via the phosphatidylinositol-3 kinase-dependent pathway in canine hearts. Cardiovasc Drugs Ther. 2005;19:33–40.
7. Hirata A, Minamino T, Asanuma H, et al. Erythropoietin enhances neovascularization of ischemic myocardium and improves left ventricular dysfunction after myocardial infarction in dogs. J Am Coll Cardiol. 2006;48:176–84.
8. Ott I, Schulz S, Mehilli J, et al. Erythropoietin in patients with acute ST-segment elevation myocardial infarction undergoing primary percutaneous coronary intervention: a randomized, double-blind trial. Circ Cardiovasc Interv. 2010;3:408–13.
9. Voors AA, Belonje AM, Zijlstra F, et al. A single dose of erythropoietin in ST-elevation myocardial infarction. Eur Heart J. 2010;31:2593–600.
10. Najjar SS, Rao SV, Melloni C, et al. Intravenous erythropoietin in patients with ST-segment elevation myocardial infarction: REVEAL: a randomized controlled trial. JAMA. 2011;305:1863–72.
11. Ozawa T, Toba K, Suzuki H, et al. Single-dose intravenous administration of recombinant human erythropoietin is a promising treatment for patients with acute myocardial infarction—randomized controlled pilot trial of EPO/AMI-1 study. Circ J. 2010;74:1415–23.
12. Taniguchi N, Nakamura T, Sawada T, et al. Erythropoietin prevention trial of coronary restenosis and cardiac remodeling after ST-elevated acute myocardial infarction (EPOC-AMI): a pilot, randomized, placebo-controlled study. Circ J. 2010;74:2365–71.
13. Opie LH. Erythropoietin as a cardioprotective agent: down but not out. Heart. 2011;97:1537–9.
14. Vaziri ND. Thrombocytosis in EPO-treated dialysis patients may be mediated by EPO rather than iron deficiency. Am J Kidney Dis. 2009;53:733–6.
15. Baker JE, Kozik D, Hsu AK, Fu X, Tweddell JS, Gross GJ. Darbepoetin alfa protects the rat heart against infarction: dose–response, phase of action, and mechanisms. J Cardiovasc Pharmacol. 2007;49:337–45.
16. Uesaka H. A personal view of methods of sample size estimation for a clinical trial. Jpn J Biom. 2003;24:17–41.
17. Jennison C, Turnbull BW. Group sequential methods with applications to clinical trials. Boca Raton: Chapman & Hall/CRC; 2000.
18. Zhang J, Somani AK, Siminovitch KA. Roles of the SHP-1 tyrosine phosphatase in the negative regulation of cell signalling. Semin Immunol. 2000;12:361–78.
19. Kanellakis P, Pomilio G, Agrotis A, et al. Darbepoetin-mediated cardioprotection after myocardial infarction involves multiple mechanisms independent of erythropoietin receptor-common beta-chain heteroreceptor. Br J Pharmacol. 2010;160:2085–96.
20. Hausenloy DJ, Baxter G, Bell R, et al. Translating novel strategies for cardioprotection: the Hatter Workshop Recommendations. Basic Res Cardiol. 2010;105:677–86.
21. Schwartz Longacre L, Kloner RA, Arai AE, et al. New horizons in cardioprotection: recommendations from the 2010 National Heart, Lung, and Blood Institute Workshop. Circulation. 2011;124:1172–9.
22. Downey JM, Cohen MV. Why do we still not have cardioprotective drugs? Circ J. 2009;73:1171–7.
23. Piot C, Croisille P, Staat P, et al. Effect of cyclosporine on reperfusion injury in acute myocardial infarction. N Engl J Med. 2008;359:473–81.
24. Botker HE, Kharbanda R, Schmidt MR, et al. Remote ischaemic conditioning before hospital admission, as a complement to angioplasty, and effect on myocardial salvage in patients with acute myocardial infarction: a randomised trial. Lancet. 2010;375:727–34.
25. Moon C, Krawczyk M, Paik D, Lakatta EG, Talan MI. Cardioprotection by recombinant human erythropoietin following acute experimental myocardial infarction: dose response and therapeutic window. Cardiovasc Drugs Ther. 2005;19:243–50.
26. Li J, Xu H, Gao Q, Wen Y. Effect of erythropoiesis-stimulating agents in acute ST-segment elevation myocardial infarction: a systematic review. Eur J Clin Pharmacol. 2011;68:469–77.
27. Stein A, Mohr F, Laux M, et al. Erythropoietin-induced progenitor cell mobilisation in patients with acute ST-segment-elevation myocardial infarction and restenosis. Thromb Haemost. 2012;107:769–74.
28. Minamino T, Toba K, Higo S, Nakatani D, Ozawa T. Erythropoietin, progenitor cells and restenosis. A critique of Stein et al. Thromb Haemost. 2012;107:1193.
29. Carlsson M, Ubachs JF, Hedstrom E, Heiberg E, Jovinge S, Arheden H. Myocardium at risk after acute infarction in humans on cardiac magnetic resonance: quantitative assessment during follow-up and validation with single-photon emission computed tomography. JACC Cardiovasc Imaging. 2009;2:569–76.

Erythropoietin, progenitor cells and restenosis. A critique of Stein et al.

Tetsuo Minamino[1]; Ken Toba[2]; Shuichiro Higo[1]; Daisaku Nakatani[1]; Takuya Ozawa[2]

[1]Department of Cardiovascular Medicine, Osaka University Graduate School of Medicine, Suita, Niigata, Japan; [2]First Department of Internal Medicine, Niigata University Medical and Dental Hospital, Niigata, Japan

Dear Sirs,

In the recently published work by Stein et al., "Erythropoietin-induced progenitor cell mobilisation in patients with acute ST-segment-elevation myocardial infarction and restenosis" (2), the authors presented the measurements of target lesions that were analysed using quantitative coronary angiography (QCA) for patients from the Regeneration of Vital Myocardium in ST-Segment Elevation Myocardial Infarction by Erythropoietin (REVIVAL-3) study (1, 2).

In the REVIVAL-3 study, patients with ST-segment elevation myocardial infarction (STEMI) undergoing percutaneous coronary intervention (PCI) were randomly assigned to receive a high-dose of epoetin beta (EPO) (n=68) or a placebo (n=70). In a post-hoc analysis, Stein et al. investigated the effects of EPO on the target lesions following stent implantation using QCA. The authors showed that the segment diameter stenosis at six months was significantly increased in patients receiving EPO than in those receiving a placebo (32 ± 19% vs. 26 ± 14%, p=0.046), and that there was a trend towards a higher incidence of revascularisation of the infarct-related artery in the EPO group than in the placebo group (p=0.08). Therefore, the authors concluded that EPO administration was associated with an increased segmental diameter stenosis and increased target lesion revascularisation. However, readers may need to interpret the data with caution for the following reasons.

(i) Late lumen loss is often used as an efficacy end-point in clinical studies to evaluate restenosis of the target lesion because this parameter indicates the absolute loss of the minimum lumen diameter of the target lesion from the time of the stenting procedure through the follow-up period. In the REVIVAL-3 trial, the authors showed that the late lumen loss at six months tended to be lower in the EPO group than in the placebo group (2.1 ± 0.7 vs. 2.3 ± 0.6 mm, p=0.070). Consistently, two small clinical studies using low doses of EPO also demonstrated that late lumen loss did not differ between the control group and the EPO treated group; however, Stein et al. did not discuss this issue in the present study (3, 4). Because the segment diameter stenosis at six months was significantly increased in the EPO group than in the placebo group and because late lumen loss tended to be lower in the EPO group than in the placebo group, the segment diameter stenosis immediately after the completion of the stenting procedure is likely to be higher in the EPO group than in the placebo group. If this is the case, the increased segment diameter stenosis at the six-month follow-up in the EPO group could be attributable to increased residual stenosis immediately after the completion of the stenting procedure rather than to an additional increase in diameter stenosis by EPO. We would like the authors to confirm the value of late lumen loss and to list the angiographic parameters at baseline, immediately after the completion of the stenting procedure and at follow-up in their Table 2.

(ii) The authors may need to verify the results in their Table 2. The minimal lumen diameter and diameter stenosis are usually described as the mean ± standard deviation. Binary restenosis should be expressed as a number (%). In addition, to avoid treatment bias, target lesion revascularisation may need to be pre-specified as either ischaemia driven or clinically driven. Otherwise, binary restenosis may be a better measure of the actual clinical impact of EPO on neointimal proliferation.

Further studies assessing the administration of EPO to patients suffering from myocardial infarction are needed because inconsistent results have been obtained (2–6). The use of appropriate parameters and interpretation may contribute to a better understanding of how EPO affects neointimal proliferation in patients with STEMI.

Conflicts of interest

None declared.

Correspondence to:
Tetsuo Minamino, MD, PhD
Department of Cardiovascular Medicine
Osaka University Graduate School of Medicine
2–2 Yamada-oka, Suita Osaka 565–0871, Japan
E-mail: minamino@cardiology.med.osaka-u.ac.jp

Received: February 25, 2012
Accepted: March 4, 2012
Prepublished online: April 26, 2012
doi:10.1160/TH12-02-0114
Thromb Haemost 2012; 107: 1193

References

1. Stein A, Mohr F, Laux M, et al. Erythropoietin-induced progenitor cell mobilisation in patients with acute ST-segment-elevation myocardial infarction and restenosis. Thromb Haemost 2012; 107: 769-774.
2. Ott I, Schulz S, Mehilli J, et al. Erythropoietin in patients with acute ST-segment elevation myocardial infarction undergoing primary percutaneous coronary intervention: a randomized, double-blind trial. Circ Cardiovasc Interv 2010; 3: 408–413.
3. Ozawa T, Toba K, Suzuki H, et al. Single-dose intravenous administration of recombinant human erythropoietin is a promising treatment for patients with acute myocardial infarction – randomized controlled pilot trial of EPO/AMI-1 study. Circ J 2010; 74: 1415–1423.
4. Taniguchi N, Nakamura T, Sawada T, et al. Erythropoietin prevention trial of coronary restenosis and cardiac remodeling after ST-elevated acute myocardial infarction (EPOC-AMI): a pilot, randomized, placebo-controlled study. Circ J 2010; 74: 2365–2371.
5. Voors AA, Belonje AM, Zijlstra F, et al. A single dose of erythropoietin in ST-elevation myocardial infarction. Eur Heart J 2010; 31: 2593–2600.
6. Opie LH. Erythropoietin as a cardioprotective agent: down but not out. Heart 2011; 97: 1537–1539.

Circulation
JOURNAL OF THE AMERICAN HEART ASSOCIATION

American Heart Association®

Feasibility, Safety, and Therapeutic Efficacy of Human Induced Pluripotent Stem Cell-Derived Cardiomyocyte Sheets in a Porcine Ischemic Cardiomyopathy Model

Masashi Kawamura, Shigeru Miyagawa, Kenji Miki, Atsuhiro Saito, Satsuki Fukushima, Takahiro Higuchi, Takuji Kawamura, Toru Kuratani, Takashi Daimon, Tatsuya Shimizu, Teruo Okano and Yoshiki Sawa

Circulation. 2012;126:S29-S37
doi: 10.1161/CIRCULATIONAHA.111.084343
Circulation is published by the American Heart Association, 7272 Greenville Avenue, Dallas, TX 75231

Print ISSN: 0009-7322. Online ISSN: 1524-4539

Feasibility, Safety, and Therapeutic Efficacy of Human Induced Pluripotent Stem Cell-Derived Cardiomyocyte Sheets in a Porcine Ischemic Cardiomyopathy Model

Masashi Kawamura, MD; Shigeru Miyagawa, MD, PhD; Kenji Miki, MSc; Atsuhiro Saito, PhD; Satsuki Fukushima, MD, PhD; Takahiro Higuchi, MD; Takuji Kawamura, MD; Toru Kuratani, MD, PhD; Takashi Daimon, PhD; Tatsuya Shimizu, MD, PhD; Teruo Okano, PhD; Yoshiki Sawa, MD, PhD

Background—Human induced pluripotent stem cell-derived cardiomyocytes (hiPS-CMs) are a promising source of cells for regenerating myocardium. However, several issues, especially the large-scale preparation of hiPS-CMs and elimination of undifferentiated iPS cells, must be resolved before hiPS cells can be used clinically. The cell-sheet technique is one of the useful methods for transplanting large numbers of cells. We hypothesized that hiPS-CM-sheet transplantation would be feasible, safe, and therapeutically effective for the treatment of ischemic cardiomyopathy.

Methods and Results—Human iPS cells were established by infecting human dermal fibroblasts with a retrovirus carrying Oct3/4, Sox2, Klf4, and c-Myc. Cardiomyogenic differentiation was induced by WNT signaling molecules, yielding hiPS-CMs that were almost 90% positive for α-actinin, Nkx2.5, and cardiac troponin T. hiPS-CM sheets were created using thermoresponsive dishes and transplanted over the myocardial infarcts in a porcine model of ischemic cardiomyopathy induced by ameroid constriction of the left anterior descending coronary artery (n=6 for the iPS group receiving sheet transplantation and the sham-operated group; both groups received tacrolimus daily). Transplantation significantly improved cardiac performance and attenuated left ventricular remodeling. hiPS-CMs were detectable 8 weeks after transplantation, but very few survived long term. No teratoma formation was observed in animals that received hiPS-CM sheets.

Conclusions—The culture system used yields a large number of highly pure hiPS-CMs, and hiPS-CM sheets could improve cardiac function after ischemic cardiomyopathy. This newly developed culture system and the hiPS-CM sheets may provide a basis for the clinical use of hiPS cells in cardiac regeneration therapy. **(*Circulation*. 2012;126[suppl 1]:S29–S37.)**

Key Words: pluripotent stem cell ■ regeneration therapy ■ transplantation

The myocardium has limited regenerative capacity, and loss of myocardium due to myocardial infarction therefore leads to heart failure. Despite remarkable recent progress in medical and surgical treatments for heart failure, end-stage heart failure remains a leading cause of morbidity and mortality.[1] Therefore, the myocardium is one of the most important targets in regenerative medicine. Cell therapy has been introduced as a new treatment for heart failure. Clinical trials using bone marrow cells and myoblasts are underway; although these cells improve cardiac performance, chiefly through paracrine cytokine effects, they show limited differentiation into cardiomyocytes.[2]

Induced pluripotent stem (iPS) cells were first generated by nuclear reprogramming of mouse fibroblasts in 2006,[3] and human iPS (hiPS) cells were established in 2007 by the transduction of defined factors.[4,5] The production of hiPS cells poses fewer legal and ethical issues than does the generation of human embryonic stem (ES) cells. In addition, recent studies have demonstrated methods for the highly efficient production from hiPS cells of cardiomyocytes with typical electrophysiological function and pharmacological responsiveness.[6,7] Human iPS cells represent an unlimited source of cardiomyocytes because of their great potential for differentiation and are therefore one of the most promising sources of cells for cardiac regenerative therapy.[8,9] Nevertheless, many important problems, especially the large-scale preparation of cardiomyocytes by differentiation of iPS cells and the elimination of undifferentiated iPS cells to avoid teratoma formation, must be addressed before hiPS cells can be used clinically.[8,9]

The recently developed scaffoldless tissue engineering technique of cell-sheet engineering is applicable to myocar-

From the Department of Cardiovascular Surgery, Osaka University Graduate School of Medicine, Suita, Osaka, Japan (M.K., S.M., K.M., S.F., T.H., T. Kawamura, T. Kuratani, Y.S.); the Medical Center for Translational Research, Osaka University Hospital, Suita, Osaka, Japan (A.S.); the Department of Biostatistics, Hyogo College of Medicine, Nishinomiya, Hyogo, Japan (T.D.); and the Institute of Advanced Biomedical Engineering and Science, TWIns, Tokyo Women's, Medical University, Shinjuku-ku, Tokyo, Japan (T.S., T.O.).

Presented at the 2011 American Heart Association meeting in Orlando, FL, November 13–17, 2011.

The online-only Data Supplement is available at http://circ.ahajournals.org/lookup/suppl/doi:10.1161/CIRCULATIONAHA.111.084343/-/DC1.

Correspondence to Yoshiki Sawa, MD, PhD, 2-2 Yamada-oka, Suita, Osaka, 565-0871, Japan. E-mail sawa-p@surg1.med.osaka-u.ac.jp

Circulation **is available at http://circ.ahajournals.org** **DOI: 10.1161/CIRCULATIONAHA.111.084343**

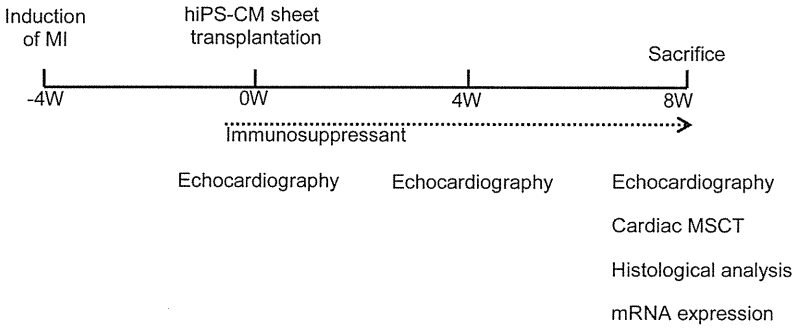

Figure 1. Study protocol of the minipig experiment and the evaluation of cardiac function and histological analysis.

dial regeneration therapy.[10] In contrast to the needle injection technique, the cell-sheet technique can deliver a large number of cells to damaged myocardium without the loss of transplanted cells or injury to the host myocardium. We have previously reported that use of the cell-sheet technique with autologous skeletal myoblasts improves cardiac function in small and large animal models of ischemic cardiomyopathy.[11,12]

We hypothesized that hiPS-derived cardiomyocyte (hiPS-CM)-sheet transplantation would be therapeutically effective in the context of ischemic cardiomyopathy. In this study, we examined the following aspects of this procedure: stable in vitro culture of a large number of cardiomyocytes by differentiation of hiPS cells, generation of hiPS-CM sheets for clinical applications using temperature-responsive dishes, survival of hiPS-CM sheets in the myocardium of a large animal, and the direct contribution of these sheets to the improvement of cardiac performance by structural and electromechanical integration into the recipient myocardium, without teratoma formation, in a porcine ischemic cardiomyopathy model.

Materials and Methods

Animal care complied with the "Guide for the Care and Use of Laboratory Animals" (National Institutes of Health publication No. 85-23, revised 1996). Experimental protocols were approved by the Ethics Review Committee for Animal Experimentation of Osaka University Graduate School of Medicine.

Culture, Differentiation, and Purification of hiPS Cells and Collection of Conditioned Medium

The hiPS cell line 201B7 that was generated using the 4 transcription factors Oct4, Sox2, Klf4, and c-Myc (a generous gift from Professor Yamanaka, Kyoto University, Kyoto, Japan) was used in this study.[4] The hiPS cells were cultured on Matrigel (BD Bioscience)-coated dishes in mTeSR1 medium (Stem Cell Technologies).

Human iPS cells were then dissociated using StemPro Accutase Cell Dissociation Reagent (Invitrogen), transferred to Corning ultralow-attachment surface culture dishes (Sigma-Aldrich) at a density of 50 000 cells/mL in mTeSR1 with Y-27632 (Wako), and cultured for 4 days to allow them to form embryoid bodies. The embryoid bodies were replated with differentiation medium (DMEM-F12; Invitrogen) containing 20% fetal bovine serum, 100 μmol/L nonessential amino acids (Invitrogen), 50 U/mL penicillin, 50 mg/mL streptomycin (Invitrogen), and 5.5 mmol/L 2-mercaptoethanol (Invitrogen) and supplemented with 100 ng/mL Wnt3a (R&D Systems) and 100 ng/mL R-Spondin-1 (Stem RD) and cultured for 2 days. The culture medium was then replaced with differentiation medium without the supplemental factors for 2 days and then changed to differentiation medium supplemented with 100 ng/mL Dkk1 (R&D Systems) for 2 days. On Day 10, the embryoid bodies were plated on gelatin-coated dishes in differentiation medium, which was refreshed every 2 days.

The culture medium was subsequently replaced with no-glucose Dulbecco modified Eagle medium (Invitrogen) with 1 mmol/L lactic acid (Wako; F. Hattori and K. Fukuda. WO2007/088874; PCT/JP2007/051563, 2007) on Day 20 and changed to Dulbecco modified Eagle medium/10% fetal bovine serum the next day. On Day 25, the culture medium was again replaced with no-glucose Dulbecco modified Eagle medium with 1 mmol/L lactic acid and changed to Dulbecco modified Eagle medium/10% fetal bovine serum the next day; this procedure eventually generated pure hiPS-CM. The hiPS-CMs were then labeled with a red fluorescent marker (CellTracker Red CMTPX; Invitrogen) as previously described.[13]

Fetal bovine serum-free Dulbecco modified Eagle medium media were conditioned by hiPS-CMs for 48 hours after the completion of our differentiation and purification protocols. A total of 48 cytokines and growth factors were measured by the Bio-Plex human cytokine assay (Bio-Rad) for in vitro screening.

Preparation of hiPS Cell-Derived Cardiomyocyte Sheets

The hiPS-CMs were detached using StemPro Accutase Cell Dissociation Reagent and seeded onto 6-cm UpCell dishes (CellSeed). The next day, the dish was incubated at room temperature, which caused the cells to detach spontaneously to form scaffold-free hiPS-CM sheets.

Generation of the Porcine Chronic Myocardial Infarction Model and hiPS-CM Sheet Transplantation

A chronic myocardial infarction model was generated by placement of an ameroid constrictor (COR-2.50-SS; Research Instruments) around the left anterior descending coronary artery in female minipigs (Japan Farm) weighing 20 to 25 kg[14] (Figure 1). Four weeks after myocardial infarction induction, transplantation of hiPS-CM sheets was performed through median sternotomy under general anesthesia. All animals were immunosuppressed with daily intake of tacrolimus (0.6 mg/kg; Astellas) from 5 days before transplantation until euthanasia. The minipigs were randomly divided into 2 treatment groups, either hiPS-CM sheet transplantation (iPS group) or sham operation (n=6 each).

Standard and 2-Dimensional Speckle-Tracking Echocardiography

Transthoracic echocardiography was performed under general anesthesia using a 5.0-MHz transducer (Aplio Artida). The left ventricular (LV) end-diastolic and end-systolic diameters were measured, whereas the LV end-diastolic and end-systolic volumes (LVEDV and LVESV, respectively) were calculated from the Teichholz formula.[15] The LV ejection fraction (LVEF) was calculated from the following formula: LVEF (%)=100×(LVEDV−LVESV)/(LVEDV).

Two-dimensional speckle-tracking echocardiography analysis was performed using the customized 2-dimensional speckle-tracking echocardiography software for the Toshiba system (2D Wall Motion Tracking). Regional cardiac function was evaluated using radial strain values obtained from the midshort-axis plane and expressed as a percentage.

Cardiac CT Scan

Electrocardiography-gated multislice CT was performed in the supine position with a 16-slice multislice CT scanner (Somatron Emotion 16; Siemens) during end-expiratory breathhold under general anesthesia. Multislice CT was performed after intravenous injection of 90 mL of nonionic contrast medium (Iomeprol; Bracco Imaging). Axial images were reconstructed using the scanner software. All images were analyzed on a workstation (AZE; Virtual Pl Lexus 64). LVEDV and LVESV were obtained from the workstation and LVEF was calculated using the formula described previously.

Holter Electrocardiography

Holter electrocardiography was performed for 24 hours in both groups (n=6 each). The arrhythmogenesis associated with hiPS-CM sheet transplantation was evaluated based on the number of premature ventricular contractions.

Histology, Immunohistolabeling, and Fluorescence In Situ Hybridization

Dissociated cultured cells were fixed in 4% paraformaldehyde. Primary antibodies included anticardiac troponin T (cTNT; Abcam), anti-Nkx2.5 (Santa Cruz Biotechnology), anti-α-actinin (Sigma-Aldrich), antihuman CD31 (BD Bioscience), antihuman CD34 (BD Bioscience) and antivimentin (BD Bioscience) visualized by fluorescent-conjugated secondary antibodies such as AlexaFluor488 goat antirabbit IgG, AlexaFluor488 goat antimouse IgG, and AlexaFluor488 donkey antigoat IgG (Invitrogen) with counterstaining by 4′6-diamidino-2-phenylindole (Dojindo) and assessed by fluorescence microscopy. Images of the samples were acquired with a Biorevo BZ-9000 (Keyence). Positivity of the cardiomyocyte-specific markers or other lineage markers in the cultured cells was determined from the acquired images by using computer-based cell counting with the Dynamic Cell Count BZ-H1CE software (Keyence).

The excised heart specimen was fixed with either 10% buffered formalin or 4% paraformaldehyde for frozen sections. Picrosirius red or periodic acid-Schiff stains were used to assess interstitial fibrosis or cardiomyocyte hypertrophy, respectively. To evaluate neovascularization in the peri-infarct area, immunolabeling with antihuman von Willebrand factor antibody (Dako) was done. The frozen sections were immunolabeled by the primary antibodies such as anticTNT (Abcam) and antislow myosin heavy chain (Sigma-Aldrich) antibodies, visualized by AlexaFluor488 goat antimouse IgG (Invitrogen), counterstained by 4′,6-diamidino-2-phenylindole, and assessed by fluorescence microscopy or confocal laser microscopy.

The hiPS-CMs at 8 weeks after transplantation were detected by fluorescent in situ hybridization using a human specific genomic probe labeled by Cy3 (Chromosome Science Labs). The samples were double-stained with other antibodies described previously and counterstained with 4′,6-diamidino-2-phenylindole.

Real-Time Polymerase Chain Reaction

Total RNA was extracted from cardiac tissue and reverse transcribed using TaqMan reverse transcription reagents (Applied Biosystems), and real-time polymerase chain reaction was performed with the ABI PRISM 7700 (Applied Biosystems) system using pig-specific primers for vascular endothelial growth factor and basic fibroblast growth factor. The average copy number of gene transcripts was normalized to that of glyceraldehyde-3-phosphate dehydrogenase for each sample.

Statistical Analysis

JMP software (JMP7.01; SAS Institute Inc) was used for all statistical analyses. Continuous values are expressed as the mean±SD. Within-group differences were compared with the Wilcoxon signed-rank test and between-group differences with the Wilcoxon-Mann-Whitney U test because the sample sizes are too small (just n=6 in each group and n=6 pairs) to allow checking of the assumptions of the unpaired and paired *t* tests, respectively. A probability value <0.05 was considered statistically significant.

Results

Generation of Highly Purified hiPS-CM Sheets

Cardiomyogenic differentiation of hiPS cells was induced by treatment of the embryoid bodies formed from cultured hiPS cells with Wnt3a and R-Spondin-1. Subsequently, the differentiated hiPS cells were purified by culture in glucose-free medium to yield hiPS-CMs. The hiPS-CMs were highly positive for the cardiomyocyte-specific markers α-actinin (89.7%±3.8%), cTNT (87.4%±4.2%), and Nkx2.5 (84.2%± 4.3%), as assessed by immunohistolabeling (Figure 2A–D). In addition, the hiPS-CMs included a small population of cells expressing vascular endothelial or endothelial progenitor cell-specific markers such as CD31 (2.9%±3.0%) and CD34 (1.6%±1.4%; Figures 2A, 2E, and 2F). These cells also included a small population of vimentin-positive cells (2.4%±1.0%), which is a marker of fibroblast or smooth muscle cells (Figures 2A and 2G).

Serum-free conditioned media from hiPS-CMs were screened for the secreted factors by using enzyme-linked immunosorbent assay (Figure 2H–I). The media contained high concentrations of various factors such as hepatocyte growth factor (HGF), stromal cell-derived factor (SDF), interluekin 6, leukemia inhibitory factor (LIF), macrophage migration inhibitory factor (MIF), and monocyte chemoattractant protein-1.

Subsequently, culture in the thermoresponsive dishes yielded round-shaped scaffold-free hiPS-CM sheets (Figure 2J). Hematoxylin & eosin-stained cross-sections of the sheet showed a 30- to 50-μm-thick regular structure with abundant extracellular matrix (Figure 2K). Immunohistolabeling showed that the cytoplasm of most of the cells in the hiPS-CM sheets was homogeneously positive for cTNT (Figure 2L).

Feasibility and Safety of hiPS-CM Sheet Transplantation Into the Chronic Myocardial Infarction Heart

Transplantation of 8 hiPS-CM sheets was successfully performed through median sternotomy under general anesthesia in 6 immunosuppressed minipigs with LVEF values of 35% to 45% due to induced chronic myocardial infarction. There was no mortality related to the procedure or otherwise before the planned euthanasia. Twenty-four-hour electrocardiography monitoring only rarely identified ventricular arrhythmias in either group before the planned euthanasia (data not shown). In addition, no teratomas were formed in the heart or other thoracic organs within the 8 weeks after the transplantation of the hiPS-CM sheets (data not shown).

Global Cardiac Functional Recovery After hiPS-CM-Sheet Transplantation

Serial standard transthoracic echocardiography was performed before and 4 and 8 weeks after the cell-sheet transplantation or sham surgery. The baseline LV end-diastolic diameter, LV end-systolic diameter, and LVEF did not differ significantly between the 2 groups. The sham-operated pigs showed nonsignificant upward trends in LV end-diastolic diameter and LV end-systolic diameter and a downward trend in LVEF between 4 and 8 weeks after surgery (Figure 3A–C). LVEF was significantly greater in the iPS group than in the sham group after 4 (53.2%±4.3% versus 38.3%±4.3%, $P<0.01$) and 8 (51.6%±4.9% versus 36.0%±5.9%, $P<0.01$) weeks. LV